

Research paper

Thiohydantoins and hydantoins derived from amino acids as potent urease inhibitors: Inhibitory activity and ligand-target interactions

Priscila Goes Camargo^a, Marciéli Fabris^a, Matheus Yoshimitsu Tatsuta Nakamae^a, Breno Germano de Freitas Oliveira^b, Camilo Henrique da Silva Lima^c, Ângelo de Fátima^b, Marcelle de Lima Ferreira Bispo^a, Fernando Macedo Jr.^{a,*}

^a Department of Chemistry, Center of Exact Sciences, State University of Londrina, Londrina, PR, Brazil

^b Department of Chemistry Institute of Exact Sciences, Federal University of Minas Gerais, Belo Horizonte, MG, Brazil

^c Chemistry Institute, Federal University of Rio de Janeiro, Rio de Janeiro, RJ, Brazil

ARTICLE INFO

Keywords:

Thiohydantoins
Hydantoins
NMR
Molecular docking
C. ensiformis
STD

ABSTRACT

We report the investigation of hydantoins and thiohydantoins derived from *L* and *D*-amino acids as inhibitors against the *Canavalia ensiformis* urease (CEU). The biochemical *in vitro* assay against CEU revealed a promising inhibitory potential for most thiohydantoins with six of them showing %I higher than the reference inhibitor thiourea (56.5%). In addition, thiohydantoin derived from *L*-valine, **1b**, as well as the hydantoin **2d**, derived from *L*-methionine, were identified as the most potent inhibitors with %I = 90.5 and 85.9 respectively. Enzyme kinetic studies demonstrated a mixed and uncompetitive inhibition profile for these compounds with K_i values of 0.42 mM for **1b** and 0.99 mM for **2d**. These kinetic parameters, obtained from traditional colorimetric assay, were strictly related to the K_D values measured spectroscopically by the Saturation Transfer Difference (STD) technique for the urease complex. STD was also used to evince the moieties of the ligands responsible for the binding with the enzyme. Molecular docking studies showed that the thiohydantoin and hydantoin rings can act as a pharmacophoric group due to their binding affinity by hydrogen bonding interactions with critical amino acid residues in the enzyme active and/or allosteric site. These findings agreed with the experimental alpha values, demonstrating that **1b** has affinity by free enzyme, and **2d** derivative, an uncompetitive inhibitor, has great binding affinity at the allosteric site. The results for the thiohydantoin **1a**, derived from *D*-valine, demonstrated a drastic stereochemical influence on inhibition, kinetics, and binding parameters in comparison to its enantiomer **1b**.

1. Introduction

Ureases (EC 3.5.1.5) are a group of metalloenzymes belonging to the family of amidohydrolases and phosphotriesterases. Among other binuclear metallohydrolases, ureases are the only ones to have Ni^{2+} ions in the active site [1]. They are prevalent among plants, algae, fungi, and bacteria but not found in animals. Regardless of the organism, ureases have as their main function the hydrolysis of urea, resulting in carbamate and ammonia as products, being able to accelerate the rate of this reaction at least 10^{14} compared to urea decomposition by an elimination reaction [2].

Their pivotal environmental role is to allow the organism to use urea (natural substrate) as a source of nitrogen. In addition, ureases participate in systemic nitrogen transport pathways, acting as a toxin for plant

defense. Pathogenic microorganisms use ammonia released from the ureases catalytic activity to neutralize the gastric environment in infected mammals [3]. Therefore, the applicability of urease is broad and includes agriculture and medicine.

The amount of nitrogen available in agriculture comes from the atmosphere since, in the soil, this nutrient can be lost by leaching, denitrification, and volatilization [4]. An alternative to increase the amount of nitrogen available to plants is the use of urea-based fertilizers [5], on the other hand, the effectiveness of using urea as a fertilizer is impaired due to the hydrolysis process caused by the catalytic activity of urease present in the soil, resulting in the emission of ammonia which, its volatilization also contributes to the pollution and degradation of ecosystems near the sites of application [6].

In the medical context, infections by ureolytic bacteria, such as

* Corresponding author.

E-mail addresses: priscilacmg@uel.br (P.G. Camargo), macedofc@uel.br (F. Macedo).

<https://doi.org/10.1016/j.cbi.2022.110045>

Received 1 March 2022; Received in revised form 10 June 2022; Accepted 13 July 2022

Available online 16 July 2022

0009-2797/© 2022 Elsevier B.V. This article is made available under the Elsevier license (<http://www.elsevier.com/open-access/userlicense/1.0/>).

Helicobacter pylori, which infects about 40–70% of the global population, cause health complications due to gastric inflammation and the development of duodenal gastric ulcers, gastric adenocarcinoma, and lymphoma [7]. This Gram-negative bacteria can survive in an acid environment, such as the stomach (pH 1–2), using urease as a defense mechanism, since the increase in local pH caused by the resulting accumulation of NH_3 by urea hydrolysis allows a favorable microenvironment for the microorganism to survive and colonize in these extreme conditions [8,9].

Therefore, both in the agro-industrial or medicinal context, alternatives in the development of urease inhibitors have great relevance. The development of enzyme inhibitors based on the structure of the natural substrate urea is a common approach used in the rational design of anti-bacterial drugs as well as to be used as an additive in urea-based fertilizers. In the last ten years, five main classes of urease inhibitors have been reported: phosphoramidites, barbiturate analogs, five- or six-membered heterocycles, and thiourea derivatives [8].

In a previous study, our research group reported the inhibitory activity of *Canavalia ensiformis* urease by benzoylthioureas [10]. These findings instigated led us to evaluate two other classes of heterocyclic compounds: 2-thioxo-imidazolidin-4-one (**1a-o**) and imidazolidin-2,4-dione (**2b-n**), commonly called, respectively, as thiohydantoins and hydantoins (Fig. 1) as potential urease inhibitors. Thiohydantoins and hydantoins can be readily synthesized [11] and are promising compounds in drug discovery because of the wide range of previously reported biological activities such as anticancer [12], antifungal [13], antioxidant [14], and antileishmanial [10,15,16]. Additionally, these compounds are reported to have low toxicity to mammalian cells ($\text{CC}_{50} = 935.7 \mu\text{g/mL}$) [17].

Therefore, to conduct a preliminary structure-activity relationship study, aliphatic, aromatic, or polar groups were introduced as side chains, and the respective thiohydantoins and hydantoins were assayed against *Canavalia ensiformis* urease. Besides, the kinetic studies and possible molecular modes of interactions of the most active compounds

were investigated experimentally by NMR using the Saturation Transfer Difference (STD) technique and theoretically by molecular docking (Fig. 1).

2. Materials and methods

2.1. Synthesis of thiohydantoins and hydantoins

2.1.1. General

Analytical grade solvents were used without previously purification. The melting points (Mp.) were determined on hot plate apparatus Microquímica (model MQAPF 302) and were not corrected. The ^1H and ^{13}C Nuclear Magnetic Resonance (NMR) spectra were acquired in a Bruker spectrometer model Avance III, operating at 400.13 MHz for ^1H and 100.13 MHz for ^{13}C , at 25 °C temperature, equipped with a 5 mm multinuclear probe. Water (D_2O , 4.70 ppm) and dimethylsulfoxide ($\text{DMSO}-d_6$, 2.50 ppm) were used as deuterated solvents and tetramethylsilane (TMS, 0.00 ppm) as the internal standard. The multiplicity of protons in the ^1H NMR spectra is reported as singlet (s), broad singlet (br), doublet (d), double doublet (dd), triplet (t), quartet (q), quintet (qt), and multiplet (m). Coupling constants (J) are reported in Hz.

2.1.2. Synthesis of thiohydantoins (**1a, 1f, and 1n**) and hydantoins (**2b-g**) from direct condensation of L or D-amino acids with urea or thiourea (Adapted from Wang et al., 2006)

In a round-bottom flask, the L or D-amino acid (20 mmol) and urea or thiourea (60 mmol) were added and heated on a sand bath at 170–180 °C for 35 min under magnetic stirring. The reactions were followed by thin-layer chromatography, using ethyl acetate as eluent and potassium permanganate. After consumption of the starting material, the mixture was allowed to cool, and then, 20 mL of distilled ice-cold water was added. The mixture was again heated until the solids formed during cooling had dissolved, and then cooled in a refrigerator for 24 h. The crystallized product formed was filtered and washed with

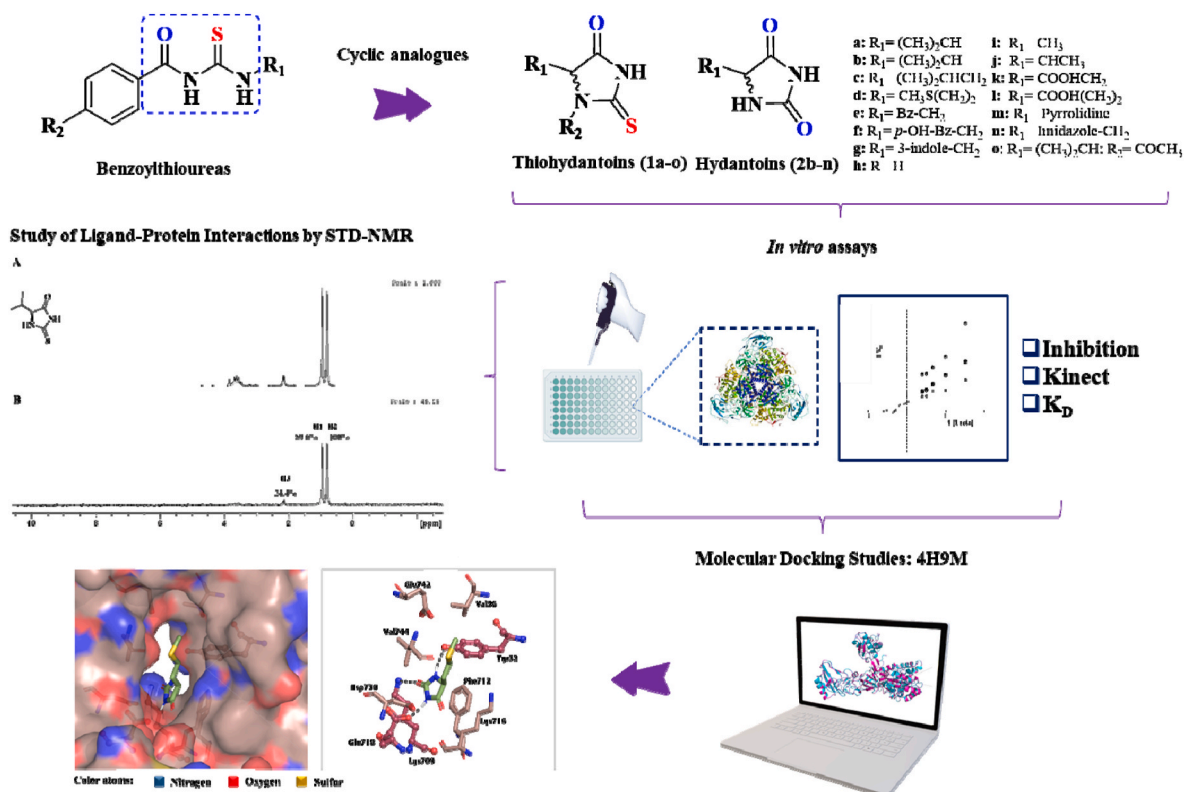


Fig. 1. The experimental approach to the anti-ureolytic evaluation, STD, and molecular docking studies of the thiohydantoins (**1a-o**) and hydantoins (**2b-n**).

ice-cold distilled water (10 mL). For substances, **2b** and **1a**, a further recrystallization process from the water were required [11].

(R)-5-Isopropyl-imidazolidin-2,4-dione (1a) (D-valine). Yield 484 mg (31%); yellow solid; Mp 139–140 °C; ¹H NMR (400.13 MHz, DMSO-*d*₆) δ 0.81 (d, *J* = 6.91 Hz, 3H), 0.95 (d, *J* = 7.02 Hz, 3H), 2.00–2.08 (m, 1H), 4.11 (dd, *J*₁ = 1.13; *J*₂ = 3.62 Hz, 1H), 10.0 (s, 1H), 11.6 (s, 1H); ¹³C NMR (100.13 MHz, DMSO-*d*₆) δ 16.54 (CH₃), 18.75 (CH₃), 30.42 (CH), 66.21 (CH), 176.42 (C=O), 183.36 (C=S).

(S)-5-(4-Hydroxybenzyl)-2-thioxoimidazolidin-4-one (1f) (L-tyrosine). Yield 282 mg (63%); yellow solid; Mp 197–202 °C; ¹H NMR (400.13 MHz, DMSO-*d*₆) δ 2.87 (d, *J* = 4.77 Hz, 2H), 4.46 (t, *J* = 4.71 Hz, 1H), 6.64 (dd, *J*₁ = 2.00; *J*₂ = 6.54 Hz, 2H), 6.95 (dd, *J*₁ = 2.00; *J*₂ = 6.60 Hz, 2H), 10.43 (br, 2H); ¹³C NMR (100.13 MHz, DMSO-*d*₆) δ 35.30 (CH₂), 62.15 (CH), 115.38 (CH), 125.32 (CH), 131.05 (C), 156.66 (C=O), 176.26 (C=O), 182.68 (C=S).

(S)-5-((1H-Imidazole-4-yl)methyl)-2-thioxoimidazolidin-4-one (1n) (L-histidine). Yield 67.85 mg (35%); yellow solid; Mp 224–228 °C; ¹H NMR (400.13 MHz, DMSO-*d*₆) δ 2.92 (dq, *J*₁ = 4.84; *J*₂ = 15.38 Hz, 2H), 4.44 (t, *J* = 5.72 Hz, 1H), 6.80 (d, *J* = 0.96 Hz, 1H), 7.54 (d, *J* = 1.12 Hz, 1H), 9.93 (s, 1H), 11.56 (br, 1H); ¹³C NMR (100.13 MHz, DMSO-*d*₆) δ 28.93 (CH₂), 61.00 (CH), 116.69 (CH), 132.64 (CH), 135.19 (C) 176.45 (C=O), 184.36 (C=S).

(S)-5-Isopropyl-imidazolidin-2,4-dione (2b) (L-valine). Yield 1200 mg (39%); yellow solid; Mp 145–146 °C; ¹H NMR (400.13 MHz, DMSO-*d*₆) δ 0.79 (d, *J* = 6.79 Hz, 3H), 0.94 (d, *J* = 6.96 Hz, 3H), 1.95–2.02 (m, 1H), 3.90 (dd, *J*₁ = 1.14; *J*₂ = 3.43 Hz, 1H), 7.92 (s, 1H) 10.6 (s, 1H); ¹³C NMR (100.13 MHz, DMSO-*d*₆) δ 16.29 (CH₃), 19.01 (CH₃), 29.99 (CH), 63.20 (CH), 158.3 (C=O), 175.9 (C=O).

(S)-5-Isobutyl-imidazolidin-2,4-dione (2c) (L-leucine). Yield 2250 mg (72%); yellow solid; Mp 215–216 °C; ¹H NMR (400.13 MHz, DMSO-*d*₆) δ 0.88 (t, *J* = 6.60 Hz, 6H), 1.35–1.52 (m, 2H), 1.72–1.82 (m, 1H), 4.00 (ddd, *J*₁ = 0.95; *J*₂ = 4.42 Hz, 1H), 10.08 (br, 1H), 11.69 (s, 1H); ¹³C NMR (100.13 MHz, DMSO-*d*₆) δ 21.91 (CH₃), 23.54 (CH₃), 24.57 (CH₂), 41.16 (CH), 56.61 (CH), 157.95 (C=O), 177.09 (C=O).

(S)-5-(2-(Methylthio)ethyl)-imidazolidin-2,4-dione (2d) (L-methionine). Yield 1720 mg (49%); yellow solid; Mp 104–105 °C; ¹H NMR (400.13 MHz, DMSO-*d*₆) δ 1.71–1.80 (m, 1H), 1.88–1.97 (m, 1H), 2.03 (s, 3H), 2.50–2.54 (m, 2H), 4.09 (dd, *J* = 4.70 Hz, 1H), 8.00 (s, 1H), 10.6 (s, 1H); ¹³C NMR (100.13 MHz, DMSO-*d*₆) δ 14.88 (CH₃), 29.18 (CH₂), 31.32 (CH₂), 57.01 (CH), 157.89 (C=O), 176.40 (C=O).

(S)-5-Benzyl-imidazolidin-2,4-dione (2e) (L-phenylalanine). Yield 3120 mg (82%); yellow solid; Mp 183–185 °C; ¹H NMR (400.13 MHz, DMSO-*d*₆) δ 2.93 (d, *J* = 4.87 Hz, 2H), 4.33 (t, *J* = 4.59 Hz, 1H), 7.16–7.29 (m, 5H), 7.92 (s, 1H), 10.4 (s, 1H); ¹³C NMR (100.13 MHz, DMSO-*d*₆) δ 36.71 (CH₂), 58.86 (CH), 127.17 (CH), 128.56 (CH), 130.20 (CH), 135.93 (C), 157.61 (C=O), 175.75 (C=O).

(S)-5-(4-Hydroxybenzyl)-imidazolidin-2,4-dione (2f) (L-tyrosine). Yield 3710 mg (90%); yellow solid; Mp 258–259 °C; ¹H NMR (400.13 MHz, DMSO-*d*₆) δ 2.81 (d, *J* = 4.83 Hz, 2H), 4.24 (t, *J* = 4.52 Hz, 1H), 6.65 (d, *J* = 8.55 Hz, 2H), 6.96 (d, *J* = 8.46 Hz, 2H), 7.85 (s, 1H), 9.34 (br, 1H), 10.22 (br, 1H); ¹³C NMR (100.13 MHz, DMSO-*d*₆) δ 36.03 (CH₂), 59.12 (CH), 115.33 (CH), 125.95 (CH), 131.15 (C), 156.55 (C=O), 157.65 (C=O), 175.77 (C=O).

(S)-5-((1H-Indol-3-yl)methyl)-imidazolidin-2,4-dione (2g) (L-tryptophane). Yield 3700 mg (81%); yellow solid; Mp 209–210 °C; ¹H NMR (400.13 MHz, DMSO-*d*₆) δ 10.9 (s, 1H), 10.4 (s, 1H), 7.89 (s, 1H), 7.55 (d, *J* = 7.87 Hz, 1H), 7.32 (d, *J* = 8.03 Hz, 1H), 7.13 (d, *J* = 2.25 Hz, 1H), 7.06 (m, 1H), 7.31–7.33 (m, 1H), 7.11 (d, *J* = 2.37 Hz, 1H), 7.04–7.08 (m, 1H), 6.97 (m, 1H), 6.95–7.00 (m, 1H), 4.30–4.32 (m, 1H), 3.07 (d, *J* = 4.89, 2H); ¹³C NMR (100.13 MHz, DMSO-*d*₆) δ 176.23 (C=O), 157.87 (C=O), 136.36 (C), 127.97 (C), 124.61 (C), 121.30 (CH), 119.06 (CH), 118.79 (CH), 111.71 (CH), 108.44 (CH), 58.78 (CH), 26.99 (CH₂).

2.1.3. Synthesis of hydantoins (2h–n) from the reaction of L-amino acids with sodium cyanate (Adapted from Schörghuber et al., 2015)

In a round-bottom flask, a mixture of L-amino acid (5.00 mmol) and

NaOCN (6.60 mmol) in water (3.00 mL) was heated at 100 °C for 3 h under magnetic stirring. After cooling to 0 °C, 6 M aqueous HCl solution (3.00 mL) was added slowly to the reaction mixture, which was heated at 120 °C for further 4 h. The reactions were followed by thin-layer chromatography, using ethyl acetate as eluent, and potassium permanganate developer. After consumption of the starting material, the solvent was reduced by evaporation on a hot plate until almost dry and the residue was cooled in a refrigerator for 24 h. After this period, the formed precipitate was filtered, washed with ice-cold distilled water (3.00 mL) giving the hydantoins of interest without the need for further purification. Compounds **2j** and **2m**, to which no precipitation was the observed product, were extracted with ethyl acetate (3 × 10 mL). The organic phase was dried with anhydrous sodium sulfate and evaporated in a rotary evaporator, resulting in the desired products without the need for further purification [18].

Imidazolidin-2,4-dione (2h) (Glycine). Yield 37 mg (62%); white solid; Mp. 221–222 °C; ¹H NMR (400.13 MHz, DMSO-*d*₆) δ 3.85 (s, 2H), 7.72 (s, 1H), 10.7 (s, 1H); ¹³C NMR (100.13 MHz, DMSO-*d*₆) δ 47.69 (CH₂), 158.88 (C=O), 174.53 (C=O).

(S)-5-Methyl-imidazolidin-2,4-dione (2i) (L-alanine): Yield 140 mg (24%); white solid; Mp 167–168 °C; ¹H NMR (400.13 MHz, DMSO-*d*₆) δ 1.21 (d, *J* = 6.92 Hz, 3H), 4.02 (dq, *J*₁ = 1.10; *J*₂ = 6.92 Hz, 1H), 7.87 (s, 1H), 10.56 (s, 1H); ¹³C NMR (100.13 MHz, DMSO-*d*₆) δ 17.70 (CH₃), 53.72 (CH), 157.57 (C=O), 177.28 (C=O).

(S)-5-(Z)-5-Ethylidene-imidazolidin-2,4-dione (2j) (L-treonine). Yield 567 mg (90%); white cristal; Mp 208–209 °C; ¹H NMR (400.13 MHz, DMSO-*d*₆) δ 1.13 (d, *J* = 6.53 Hz, 3H), 3.83 (dd, *J*₁ = 0.83; *J*₂ = 2.44 Hz, 1H), 3.90 (dq, *J*₁ = 2.62; *J*₂ = 6.50, 1H), 7.86 (s, 1H), 10.4 (s, 1H); ¹³C NMR (100.13 MHz, DMSO-*d*₆) δ 20.74 (CH₃), 64.27 (CH), 65.64 (C), 158.63 (C=O), 175.21 (C=O).

(S)-5-Acetamide-2,4-imidazolidin-4-one (2k) (L-asparagine). Yield 185 mg (23%); white solid; Mp 224–225 °C; ¹H NMR (400.13 MHz, DMSO-*d*₆) δ 2.62 (d, *J* = 5.25 Hz, 2H), 4.20 (m, 1H), 7.85 (s, 1H), 10.6 (s, 1H), 12.5 (s, 1H); ¹³C NMR (100.13 MHz, DMSO-*d*₆) δ 35.88 (CH₂), 54.79 (CH), 158.08 (C=O), 171.48 (C=O), 175.85 (C=O).

(S)-5-Propanamide-2,4-imidazolidin-4-one (2l) (L-glutamine). Yield 26 mg (23%); white solid; Mp 184–185 °C; ¹H NMR (400.13 MHz, DMSO-*d*₆) δ 1.68 (m, 1H), 1.91 (m, 1H), 2.32 (m, 1H), 4.03 (m, 1H), 8.01 (s, 1H), 10.7 (s, 1H), 12.2 (s, 1H); RMN de ¹³C (100.13 MHz, DMSO-*d*₆) δ 27.35 (CH₂), 29.55 (CH₂), 57.15 (CH), 157.81 (C=O), 174.16 (C=O), 176.29 (C=O).

(S)-Tetrahydro-1H-pirrol[1,2-c]imidazole-1,3(2H)-dione (2m) (L-proline). Yield 178 mg (25%); white solid; Mp 153–155 °C; ¹H NMR (400.13 MHz, DMSO-*d*₆) δ 1.60–1.69 (m, 1H), 1.90–2.08 (m, 3H), 3.01–3.07 (m, 1H), 3.43–3.49 (m, 1H), 4.09–4.13 (m, 1H), 10.7 (s, 1H); ¹³C NMR (100.13 MHz, DMSO-*d*₆) δ 27.13 (CH₂), 27.19 (CH₂), 45.39 (CH₂), 64.47 (CH), 161.48 (C=O), 175.91 (C=O).

(S)-5-((1H-Imidazole-4-yl)methyl)-imidazolidin-2,4-dione (2n) (L-histidine). Yield 2370 mg (26%); yellow solid; Mp 256.5 °C decomp.; ¹H NMR (400.13 MHz, D₂O) δ 3.27 (dq, *J*₁ = 5.18; *J*₂ = 15.66 Hz, 2H), 4.59 (t, *J* = 5.41 Hz, 1H), 7.34 (s, 1H), 8.65 (d, *J* = 1.32 Hz, 1H); ¹³C NMR (100.13 MHz, DMSO-*d*₆) δ 25.80 (CH₂), 57.64 (CH), 117.53 (CH), 127.11 (CH), 133.75 (C), 159.18 (C=O), 176.72 (C=O).

2.1.4. Synthesis of thiohydantoins (1k–l and 1o) from the reaction of L-amino acids with ammonium thiocyanate (Adapted from Burgess & Reyes, 2006)

In a round-bottom flask, a mixture of the suitable L-amino acid (13.3 mmol), ammonium thiocyanate (13.3 mmol), and acetic anhydride (79.3 mmol) was heated at 100 °C for 30 min under magnetic stirring. The mixture was allowed to cool down and, then ice-cold distilled water (20 mL) was added. Following, the mixture was stored at 5 °C for 24 h, the crystals were removed by vacuum filtration and the crude product was purified by recrystallization from water resulting in the acetyl thiohydantoins **1k**, **1l**, and **1o**. The corresponding acetyl-thiohydantoins **1k** and **1l** (1 mmol) was added to 10 mL of hydrochloric acid solution

(5 M) and placed in a round-bottom flask and heated at 110 °C for 60 min under magnetic stirring. The mixture was allowed to cool down to room temperature and, then the resulting in a yellow solution was extracted (3 × 10 mL) with ethyl acetate. The organic phase was dried with anhydrous sodium sulfate and evaporated in a rotary evaporator, resulting in the product of deacetylation [19].

(S)-5-Acetamide-2-thioxoimidazolidin-4-one (1k) (L-asparagine). Yield 146,38 mg (51%); yellow solid; Mp 210–212 °C; ¹H NMR (400.13 MHz, DMSO-*d*₆) δ 2.69 (s, 3H), 2.75 (dd, *J*₁ = 2.89; *J*₂ = 16.45 Hz, 1H), 3.08 (dd *J*₁ = 5.21; *J*₂ = 16.45 Hz, 1H), 4.76 (dd, *J*₁ = 2.89; *J*₂ = 5.21 Hz, 1H), 6.90 (s, 1H), 7.43 (s, 1H), 12.53 (s, 1H); RMN de ¹³C (100.13 MHz, DMSO-*d*₆) δ 27.82 (CH₃), 34.86 (CH₂), 60.07 (CH), 79.64 (C=O), 170.26 (C=O), 173.48 (C=O), 183.81 (C=S).

(S)-5-Propanamide-2-thioxoimidazolidin-4-one (1l) (L-glutamine). Yield 165 mg (80%); white solid; Mp 115–116 °C; ¹H NMR (400.13 MHz, DMSO-*d*₆) δ 1.04 (qt, *J* = 7.48 Hz, 1H), 1.93 (m, 1H), 2.34 (t, *J* = 7.35, 2H), 4.23 (t, *J* = 7.40, 1H), 10.1 (s, 1H), 11.7 (s, 1H); ¹³C NMR (100.13 MHz, DMSO-*d*₆) δ 26.66 (CH₂), 29.34 (CH₂), 60.17 (CH), 173.88 (C=O), 176.75 (C=O), 183.23 (C=S).

(S)-1-Acetyl-5-isopropyl-2-thioxoimidazolidin-4-one (1o) (L-valine). Yield 111,20 mg (42%); white solid; Mp 100–103 °C; ¹H NMR (400.13 MHz, DMSO-*d*₆) δ 0.76 (d, *J* = 6.92 Hz, 3H), 1.08 (d, *J* = 7.04 Hz, 3H), 2.39–2.47 (m, 1H), 2.73 (s, 3H), 4.58 (d, *J* = 3.40 Hz, 1H), 12.63 (br, 1H); ¹³C NMR (100.13 MHz, DMSO-*d*₆) δ 15.84 (CH₃), 17.92 (CH₃), 27.78 (CH₃), 29.39 (CH), 67.18 (CH), 170.19 (C=O), 172.67 (C=O), 183.34 (C=S).

2.2. Alpha-D measurements

Samples of the compounds **1a** (*c* = 0,020 g/mL), **1b**, and **2d** (*c* = 0,033 g/mL) were weighed and dissolved in dimethylsulfoxide, the molecular optical rotation was measured at 589 nm with a polarimeter (Biosystem, model WGX-4, sodium lamp) equipped with a cell of 100 mm. Results are available in Section B on Support Information.

2.3. In vitro assays of *Canavalia ensiformis* urease

2.3.1. Inhibitory activity test

The analysis of the inhibitory activity of the urease of CEU (*Canavalia ensiformis* - Jack Bean; Type III, CAS 9002-13-5) acquired from Sigma Aldrich Brazil (Barueri, SP-BR) was performed in triplicate, using the indophenol colorimetric methodology adapted from Khan et al. (2017) [20]. In a 96-well plate, the reaction mixture was prepared by addition of 10 µL of test compound (5.00 mM), 55.0 µL of sodium phosphate buffer solution (100 mM, pH 7.4) supplemented with EDTA (ethylenediamine tetraacetic acid, 1 mM), 100 µL of urea (10 mM) and 25.0 µL of enzymatic urease solution (0.0035 mM), which were incubated at 45 °C for 30 min. After this period, 40.0 µL of phenol reagent (1% phenol and 0.05% sodium nitroprusside) and 40.0 µL of alkaline reagent (1.0% NaOH and 0.1% sodium hypochlorite) were added to each well, and the mixture remained at rest for 15 min. The final absorbance of the reaction mixture was recorded at 630 nm with a UV–visible microplate reader Biotek (Winooski, VT, USA) model Synergy HT. The percentage of inhibition (%I) was determined by the equation:

$$\%I = 100 - \left(\left(\frac{Abs\ a}{Abs\ c} \right) \times 100 \right)$$

where **Abs a** is the observed absorbance for the samples, and **Abs c** is the observed absorbance for the control. The inhibitor standard used was thiourea (5.00 mM). Control wells contained dimethylsulfoxide (DMSO) (10.0 µL) which was the solvent used to dissolve the compounds.

2.3.2. Enzymatic kinetic test

The reaction mixture used was the same as for inhibition measurement. However, two concentrations of the test compound (2.00 and

1.00 mM) and five different concentrations of urea substrate (0.66, 1.00, 1.50, 2.00, and 2.50 mM) were used for each sample. The final absorbance of the reaction mixture was recorded at 630 nm with a UV–visible microplate reader Biotek (Winooski, VT, USA) model Synergy HT. Michaelis-Menten and Lineweaver-Burk plots were recorded, and values for inhibition constants (*K_i*) were determined using the slopes of each line graph, using the Graph-Pad software (version 8.00). The kinetics were studied by taking the reciprocal of enzymatic activity along the y-axis and the reciprocal of substrate concentration along the x-axis. The enzymatic activity was calculated through an ammonium chloride calibration curve. The tests were conducted in triplicate.

2.4. Ligand-protein interactions studies by STD

2.4.1. Sample preparation

Canavalia ensiformis urease (CEU), was used in the experiments. A stock solution of CEU (0.05 mM) was prepared in a phosphate buffer in D₂O (75 mM sodium phosphate, 150 mM sodium chloride, pH 7.50). For all ligands, 5 mM stock solutions in D₂O were prepared not exceeding the value of 1% DMSO-*d*₆ for solubilization of the compounds in the final volume. Samples for NMR analysis were prepared from these stock solutions.

2.4.2. Details and general Settings for STD experiments

The STD experiments were performed following the methodology adapted from Viegas et al. (2011), performed in a Bruker Advance III spectrometer operating at 400.13 MHz for ¹H at 25 °C, equipped with a 5 mm multinuclear probe. STD spectra were obtained using standard pulse sequence parameters provided by Bruker® (*stdiffesgp.3*), recorded with 64 scans. For each experiment, the 90° pulse was calibrated separately. For saturation of the ¹H protein nuclei (f2 channel), 50 ms selective Gaussian pulses were used with *n* repetitions throughout the saturation time ranging from 0.50 to 2.50 s, while the delay between scans was set to saturation time + 1. Suppression of protein signal was performed using a 10 ms spin-lock filter. Irradiation frequencies were set up as 400 Hz (1 ppm, on resonance) and 50,000 Hz (125 ppm, off-resonance). The suppression of the residual water signal was performed using excitation sculpting with gradients and a calibrated Sinc1.1000 pulse with 2.00 ms width [21]. The difference spectrum was obtained by subtracting the selectively irradiated spectrum from the reference spectrum.

2.4.3. Saturation time optimization for Group Epitope Mapping experiments

The samples were prepared by adding 200 µL of the CEU stock solution (0.05 mM), 100 µL of phosphate buffer in D₂O (75 mM sodium phosphate, 150 mM sodium chloride, pH 7.50), and 200 µL of the test compound stock solution (5 mM). Therefore, the final ligand-enzyme ratio (L/E) = 100. Nine experiments were acquired varying the saturation times from 0.50 to 2.50 s.

2.4.4. Longitudinal relaxation (T1) for Group Epitope Mapping experiments

The samples were prepared by adding 200 µL of the stock solution of the test compounds **1a**, **1b**, and **2d** (5 mM), 300 µL of phosphate buffer in D₂O (75 mM sodium phosphate, 150 mM sodium chloride, pH 7.50).

The inversion-recovery experiment was performed using the “t1ir” pulse sequence provided by Bruker®.

For data acquisition, a delay of 10 s was used for the three ligands, approximately between 3 and 5 times the time of the largest T1 present in the molecule. The experiment was carried out using 10-time intervals between the 180° and 90° pulses, ranging from 0.001 to 5.000 s. The experiment was performed with 32 scans [22,23]. The spectrum obtained was then processed using the dynamic analysis tools of the TopSpin v3.6.2 software, obtaining the T1 for each of the ligand signals.

2.4.5. Kinetic studies for K_D determination by STD

The determination of K_D was performed by the acquisition of five STD experiments. The samples were prepared by adding 200 μ L of the CEU stock solution (0.05 mM), 100–260 μ L of phosphate buffer, and 40.0–200 μ L of the test compound stock solution (5 mM) (depending on the concentration of ligand ranging from 0.40, 0.80, 1.00, 1.40 or 2.00 mM). Where the solutions resulted in a 20 to 100-fold excess of binder over the enzyme concentration (0.02 mM) which was kept fixed. The values for the amplification factor were obtained by the equation:

$$A_{STD} = \frac{I_{STD}}{I_0} \times \left[\frac{L}{E} \right]$$

where I_0 is the absolute area of the signal of the reference spectrum (off-resonance), I_{STD} is the absolute area of the signal observed by the STD effect (difference spectrum), and $[L/E]$ is the ligand-enzyme ratio.

The dissociation constant (K_D) was obtained from the titration based on the STD experiments, according to the analogy of Michaelis-Menten's equation resulting in:

$$A_{STD} = \frac{\alpha_{STD}[L]}{K_D + [L]}$$

where A_{STD} is the amplification factor, α_{STD} is the maximum observed amplification factor, $[L]$ is the ligand concentration. Estimation of parameters α_{STD} and K_D for the equation were obtained by linearization method of Lineweaver-Burk using the GraphPad software (version 8.0) and Solver utility of the program Excel (Microsoft, Redmond, USA).

2.5. Molecular modelling

The crystallographic structure of the *Canavalia ensiformis* urease (PDB ID: 4H9M, resolution: 1.52 Å) was obtained from the PDB (<http://www.rcsb.org>, Protein Data Bank). The active site was centered between nickel ions with the following coordinates x: 18.7825 y: 57.8095 z: 24.1515. The Allosteric site was defined between residues Tyr32, Thr33, Val36, Gln82, His492, Asp633, Phe712, Lys716, Glu718, Glu742, and Val744 (x: 61.8344 y: 23.2354, z: 89.2500), after the FTMap server analysis (<https://ftmap.bu.edu/>).

The 3D structures of thiohydantoin and hydantoin derivatives (**1a**, **1b**, **1o**, and **2d**) were constructed in Marvin Sketch, and geometry optimization was performed using the MMFF94 (ChemAxon, <https://chemaxon.com/products/marvin>). The pose with the best score for which the fitting results were considered and selected by calculating Root Mean Squared Deviation (RMSD). RMSD values between pose solutions were performed using Discovery Studio Visualizer (Dassault Systèmes BIOVIA, Discovery Studio Modeling Environment, 2017 version, San Diego: Dassault Systèmes, 2016) [24]. The analysis of intermolecular interactions and figures were built in the Pymol program (version 3.8) [25].

Molecular docking was performed using the GOLD program (Genetic Optimization for Ligand Docking, Cambridge Crystallographic Data Centre, version 2020.1), the scoring function employed was ASP (Astex Statistical Potential) [26]. Polar hydrogen atoms were added to the protein based on the ionization inferred by the program, the number of genetic operations in each run, and other parameters were set by default. Solvents such as water and β -mercaptoethanol and phosphate ions were excluded from the structure. Fragments and conformers of the modified cysteines (CME) and the *N*-carboxyl group of carbamylated lysine (KCX) were corrected. The square-pyramidal geometry was considered for Penta-coordinated Ni^{2+} (Ni902) and octahedral geometry for hexa-coordinated Ni^{2+} (Ni901). The active and allosteric radius were defined within 12 Å and 13 Å, respectively. In addition, the ligands were subjected to 10 iterative runs. The protocol validation was made by redocking considering Root Mean Square Deviation (RMSD) < 2.00 Å.

2.6. Statistical analysis

The data were from three independent experiments each performed in triplicate and were expressed as mean \pm standard error of the mean. Statistical analyzes were performed using the GraphPad software (version 8.00) (GraphPad Software, Inc., USA, 6.00) – ANOVA, or SIS-VAR (version 5.70. Distinct letters indicate significant difference between treatments by Tukey ($P < 0.05$) or Scott-Knott ($P < 0.05$) test. Pearson's correlation analysis was performed in Microsoft Office Excel (Microsoft 365), where the linear correlation coefficient r can present the values:

$r = 1$, indicates a perfect positive correlation between the two variables,

$r = -1$, indicates a perfect negative correlation between the two variables (increasing one always decreases the other, and

$r = 0$, indicates that there is no linear dependence on each other, but the result must be investigated by other means.

3. Results and discussions

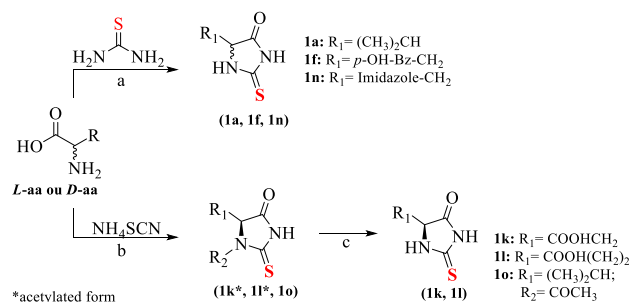
3.1. Chemistry

Ten of out fifteen thiohydantoin evaluated in this work (**1c-e**, **1e-j**, **1l-m**) were synthesized as previously described [16,17]. Thiohydantoin **1a**, **1f**, **1k**, **1l**, **1n**, and **1o**, were synthesized herein by two synthesis methods. The condensation reaction between thiourea and three different *D* or *L*-amino acids (*D*-valine, *L*-tyrosine, and *L*-histidine) Using this methodology, the derivatives **1a**, **1f**, and **1h**, were obtained in yields of 31.0%, 63.0%, and 35.0%, respectively (Table 1, entries 1, 2 and 5). The derivatives **1k**, **1l**, and **1o** were obtained in good yields by treatment of corresponding amino acid (*L*-valine, *L*-asparagine, and *L*-glutamine) with acetic anhydride and ammonium thiocyanate. **1k** and **1l** were hydrolyzed in acidic media resulting in deacetylated products with 51.0% and 80.0% yield, respectively. In addition, the acetylated compound **1o** (42.0% yield) was used for comparative purposes discussed in section 3.2 (Table 1, entries 3, 4, and 6).

The use of the methodology involving the condensation between urea and *L*-amino acids also allowed to obtain hydantoin with non-polar side chains (**2b-g**), such as valine, leucine, methionine, phenylalanine, tryptophan, and hydantoin with polar side chains such as tyrosine

Table 1

Results for the synthesis of thiohydantoin **1a**, **1f**, **1k**, **1n**, and **1o**.



Conditions: a) 170–180 °C, reflux, 35 min; b) Ac₂O, 100 °C, 30 min; c) HCl 5 M, 110 °C, 1h

Entry	Amino acids	R ₁	R ₂	Thiohydantoin	Yield (%)
1	<i>D</i> -val	(CH ₃) ₂ CH	H	1a	31
2	<i>L</i> -tyr	<i>p</i> -OH-Bz-CH ₂	H	1f	63
3	<i>L</i> -asx	COOHCH ₂	H	1k	51
4	<i>L</i> -glu	COOH(CH ₂) ₂	H	1l	80
5	<i>L</i> -his	Imidazole-CH ₂	H	1n	35
6	<i>L</i> -val	(CH ₃) ₂ CH	COCH ₃	1o	42

(30–90% yield), as shown in Table 2 (entries 1 to 6 and 13). Among the derivatives with hydrophobic side chains, those with aromatic rings **2e-g** were obtained with the highest yields ranging from 81.0 to 90.0% (Table 2, entries 4 to 6). However, this methodology failed to yield compounds derived from glycine, alanine, threonine, asparagine, glutamine, proline, and histidine, possibly due to thermic decomposition of these amino acids, or even because of side reactions involving the functional groups of their side chains, resulting in by-products [11,27].

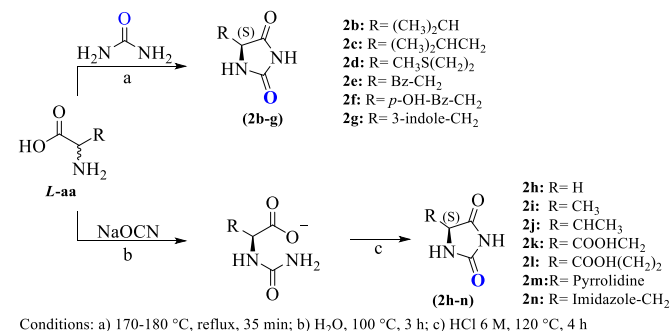
On the other hand, the methodology involving the reaction of *L*-amino acids with sodium cyanate (NaOCN) in an aqueous solution, with subsequent cyclization in the presence of chloride acid, proved to be adequate to obtain the series of hydantoin. Indeed, these conditions allowed us to obtain **2h-j** and **2m-n**, which include derivatives from amino acids with nonpolar side chains, such as alanine and proline, from polar side chains such as glycine and threonine, and from positively charged amino acids (Table 2, entries 7 to 9 and 12 to 13). The compounds (**2h-n**) were obtained with low to good yields, with the highest yield observed for the **2k** derivative of 94% (Table 2, entry 10), and the lowest yields observed for the **2i**, **2m**, and **2n** derivatives of 24, 2 and 13% respectively (Table 2, entries 8, 12 and 13).

In general, the ^1H NMR spectra of the synthesized derivatives showed chemical shift signals of the two NH groups around 7.70–12.5 ppm, in addition to signals with from 3.85 to 4.33 ppm, attributed to α -hydrogens. The ^{13}C NMR spectra showed characteristic C=O and C=S signals of the hydantoin or thiohydantoin rings at 157.6–177.3 and 182.7–183.4 ppm, respectively (Support Information, Figs. S1–19). All NMR signals of the derivatives were in agreement with the data available in the literature for these compounds [11,17,27].

3.2. Measurement of urease inhibitory activity by colorimetric technique

Thiohydantoin and hydantoin, derived from different amino acids, were used to evaluate the influence of the polar, non-polar, aliphatic, and aromatic side chains and the variation of oxygen and sulfur of the hydantoin moiety on the urease inhibition. The results of the enzyme inhibition assay revealed that all thiohydantoin (**1a-o**) inhibited urease

Table 2
Results for the synthesis of hydantoin **2b-n**.



Entry	Amino acids	R	Hydantoin	Yield (%)
1	<i>L</i> -val	$(\text{CH}_3)_2\text{CH}$	2b	39
2	<i>L</i> -leu	$(\text{CH}_3)_2\text{CHCH}_2$	2c	72
3	<i>L</i> -met	$\text{CH}_3\text{S}(\text{CH}_2)_2$	2d	49
4	<i>L</i> -phe	Bz-CH_2	2e	82
5	<i>L</i> -tyr	$p\text{-OH-Bz-CH}_2$	2f	90
6	<i>L</i> -trp	3-indole- CH_2	2g	81
7	Gly	H	2h	62
8	<i>L</i> -ala	CH_3	2i	24
9	<i>L</i> -tre	CH_3CH	2j	90
10	<i>L</i> -asx	COOHCH_2	2k	94
11	<i>L</i> -glu	$\text{COOH}(\text{CH}_2)_2$	2l	23
12	<i>L</i> -pro	Pyrrolidine	2m	25
13	<i>L</i> -his	Imidazole- CH_2	2n	13

with inhibition percentages (%I) ranging from 22 to 90%, as shown in Table 3.

Thiohydantoin **1b** had the most significant inhibitory effect of the series with %I = 90, almost twice as much as the standard inhibitor, thiourea (56%). This data evinces that the introduction of the thiohydantoin ring has a determinant positive influence on the inhibitory activity since the amino acid *L*-valine presented %I = 42, less than half of its corresponding thiohydantoin derivative.

Moreover, it is noteworthy that the thiohydantoin **1a**, derived from *D*-valine, presented a three times lower percentage of inhibition (%I = 28) than its antipode **1b**. This evidence suggests that the configuration at C5 of thiohydantoin **1a/b** displays an important stereoselective influence on the active site of the enzyme. The introduction of the acetyl group at N^1 of the thiohydantoin ring also negatively influenced the enzymatic inhibition since **1o** showed %I = 29.

The glycine derivative, **1h** presented %I = 53%, equivalent to thiourea (%I = 56), not differing statistically. It was possible to observe a good inhibitory profile showing %I = 48 to 60 for amino acid derivatives with smaller aliphatic side chains, up to three carbons such as **1h**, **1i**, and **1j** (Table 3, entries 8–10). This interpretation is supported by the lower activity observed for derivatives with a large aliphatic (**1c** and **1m**) and/or aromatic (**1e-g**) side chains (%I = 22 to 40). The derivatives **1d** (sulfur chain), **1k** (polar chain), **1n** (basic chain), and **1o** (acetylated derivative) showed good inhibition of CEU with %I = 62–69% values.

It was observed that the replacement of sulfur by oxygen in the hydantoin ring did not contribute positively to the inhibitory activity, since only seven hydantoin showed an inhibitory profile, six of them, **2i**, **2j**, **2k**, and **2l**, with %I value ranging from 3 to 10%. Hydantoin **2d**, the only one in the series with a sulfur atom in the side chain, showed %I = 86, equivalent to thiohydantoin **1b**. This finding suggests that the sulfur atom present in this derivative may be responsible for its high rate of enzymatic inhibition of CEU.

3.2.1. Study of the kinetic mechanism of urease inhibition by hydantoin and thiohydantoin

Thiohydantoin **1b**, the most active in the series with %I = 90, its enantiomer **1a** (%I = 28), and the derivative from methionine **1d** (%I = 86) were selected for additional tests with the enzyme CEU to investigate the mechanism of inhibition in the presence of different concentrations of inhibitors to study the enzyme kinetics. Michaelis-Menten and Lineweaver-Burk plots were performed, and inhibition constants values (K_i) were determined using the slopes of each line graph (Fig. 2). A plot of initial rate (V_0) versus urea concentration obtained from **1b** assay data is shown in Fig. 2A to exemplify the Michaelis-Menten behavior of enzymatic urease catalysis.

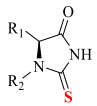

The Lineweaver-Burk plots (Fig. 2B and C) indicate that compounds **1a** and **1b** presented mixed-type inhibition against CEU urease since the lines intersect the Y-axis at different places in the second quadrant of the X-axis. The profile observed for compound **2d** presents an uncompetitive inhibition against CEU (Fig. 2D) since the lines intersect the Y and X axes in different places and are shown to be parallel.

The compound **1b** inhibited the CEU presenting $K_i = 0.4$ mM, followed by the derivative **1a** presented the highest K_i value with 1.1 mM. These compounds showed K_m values of 1.6 mM and V_{\max} ranging from 760 to 788 μmol of NH_4^+ per minute per milligram of protein (Table 4). In the case of mixed inhibitors, in addition to the parameters of inhibition constant, Michaelis-Menten constant, and maximum enzyme velocity, the alpha parameter (α) was also determined, which value corresponds to the degree binding of the inhibitor that changes the affinity of the enzyme by the substrate. Its value is always greater than zero [28].

If the value of $\alpha > 1$, the inhibitor preferentially binds to the free enzyme, which was observed for **1b**, the more active in the series (%I = 90 and $K_i = 0.4$ mM) and with $\alpha = 1.8$. Furthermore, if the alpha value is substantially higher, the binding is almost entirely to the free enzyme, a behavior observed for **1a** with $\alpha = 2.7$ [28].

Table 3

Inhibitory activity of the thiohydantoins, hydantoins, and thiourea (0.05 mM) against CEU (0.0035 mM) in a reaction containing urea as substrate (10 mM).

Entry	Amino acids	R ₁	R ₂	Thiohydantoin	%I	Hydantoin	%I
							
1	<i>D</i> -val	(CH ₃) ₂ CH	H	1a^d	28 ± 4	2a	–
2	<i>L</i> -val	(CH ₃) ₂ CH	H	1b^j	90 ± 1	2b	0
3	<i>L</i> -leu	(CH ₃) ₂ CHCH ₂	H	1c^d	33 ± 4	2c	0
4	<i>L</i> -met	CH ₃ S(CH ₂) ₂	H	1d^h	62 ± 6	2d^j	86 ± 0.3
5	<i>L</i> -phe	Bz-CH ₂	H	1e^e	41 ± 3	2e	0
6	<i>L</i> -tyr	<i>p</i> -OH-Bz-CH ₂	H	1f^d	31 ± 4	2f	0
7	<i>L</i> -trp	3-indole-CH ₂	H	1g^d	31 ± 5	2g	0
8	Gly	H	H	1h^g	53 ± 6	2h	0
9	<i>L</i> -ala	CH ₃	H	1i^b	60 ± 2	2i^a	5 ± 0.0
10	<i>L</i> -tre	CH ₃ CH	H	1j^f	48 ± 0.4	2j^a	3 ± 0.7
11	<i>L</i> -asx	COOH-CH ₂	H	1kⁱ	69 ± 2	2k^b	8 ± 2
12	<i>L</i> -glu	COOH-(CH ₂) ₂	H	1lⁱ	68 ± 4	2l^b	10 ± 1
13	<i>L</i> -pro	Pyrrolidine	H	1m^c	22 ± 0.7	2m^b	11 ± 0.3
14	<i>L</i> -his	Imidazole-CH ₂	H	1nⁱ	70 ± 3	2n^b	13 ± 3
15	<i>L</i> -val	(CH ₃) ₂ CH	COCH ₃	1o^d	29 ± 7	–	–
16	–	–	–	Thiourea^g	56 ± 2	–	–
17	<i>L</i> -val	–	–	<i>L</i>-valine^e	42 ± 6	–	–

Results represent the mean ± standard error of the mean of the experiments performed in triplicate. Different letters indicate the significant difference between treatments by the Scott-Knott test ($P < 0.05$).

For uncompetitive inhibitors, as the hydantoin **2d** ($K_i = 1.0$ mM), the product between the K_i and the α value determines the constant. Therefore, it is impossible to adjust the inhibition constant separately, as its value is extremely high compared to α since uncompetitive inhibitors generally do not bind to the free enzyme [28]. The K_m value observed was 0.6 mM and the $V_{max} = 1076 \mu\text{mol NH}_4^+$ per minute per milligram of protein (Table 4).

3.3. Study of ligand-protein interactions by STD

3.3.1. Group epitope mapping considering the relaxation of the ligand (GEM-CRL)

To investigate with more detail the interactions at the molecular level between compounds **1a**, **1b**, and **2d** with the CEU enzyme, the Saturation Transfer Difference (STD) technique was used, following the methodology adapted from Viegas et al. (2011) [29]. STD has been extensively used as an NMR tool both for screening ligands and to probe the binding sites of ligands to its macromolecule receptors (Group Epitope Mapping, GEM) [30], including studies on urease [31,32]. Since STD measures the transfer of saturation from a receptor to a ligand, an STD response reveals that a certain ligand is effectively involved in the binding process to a macromolecule, such as a protein. In addition, STD provides different response intensities to different groups of the ligand, depending on the contact distances of each group (epitopes) from the protein binding site. Since protons at different positions of the ligand molecule usually have different longitudinal relaxation times (T_1) [30, 33], it is important to use T_1 experimental values of the ligands to properly weigh the STD response [34,35] (see more details on supporting information Table S1). Therefore, considering T_1 values for each probed group of the molecule results in a STD effect that strictly relates to their proximity to the contact site.

Fig. 3A and B shown STD spectra and reference spectra (off-resonance) for the mixture of CEU (0.02 mM) and thiohydantoin **1b** (2.00 mM, L/E = 100). The intense doublets in 0.96 and 0.80 ppm (Fig. 3B) referring to the two diastereotopic methyl groups H1 and H2 respectively and H3 at 2.15 ppm referring to H β indicate, in the first instance, that this ligand is active and interacts with the enzyme. Signals in the

region of 3.40–3.91 ppm, observed in the reference spectrum (Fig. 3A), are attributed to the sugars used as stabilizers in the enzyme formulation. Since they do not present interactions with the enzyme, monitoring these resonances can be conveniently used as a negative control for the evaluation of interactions.

The highest intensity observed was set to 100% and for all other signals, the relative intensity percentage was calculated. In this way, was possible to obtain the GEM-CRL [30]. Thus, methyl H2, with a value of %STD = 100 was defined as the reference intensity parameter, consequently H1 showed %STD = 89.6 and H3 24.4% (Fig. 3B).

To evaluate the influence of the absolute configuration of **1b** (*S*) and **1a** (*R*) for the thiohydantoin derived from the amino acid valine, the STD experiment was also performed for compound **1a**. It was possible to observe the doublets in 0.96 and 0.80 ppm referring to the two diastereotopic methyl H1 and H2, respectively, showing that the compound is an active ligand for the enzyme (Fig. 4A and B).

This derivative had the highest intensity observed for methyl H1, with %STD = 100, while H2 presented 87.0% (Fig. 4B). This behavior is qualitatively contrary to that observed for *S*-enantiomer **1b**. This shows that the spatial arrangement for the valine derivative has a primordial influence on the interactions with the enzyme, since for the *in vitro* assays, it was also observed that the change from *S* to *R* configuration was reduced by three times the %I of CEU enzyme (Table 3, section 3.2).

Due to its high inhibitory activity, hydantoin **2d** was also submitted to STD studies to assess the influence of the sulphurated side chain from the methionine residue. The STD effect was observed for the singlet at 2.03 ppm, referring to methyl H4 bound to the sulfur atom, and for the methylene hydrogens, H5 at 2.55 ppm indicates an active ligand that interacts with the enzyme (Fig. 5) mainly by the terminal moiety of the linear side chain. The highest intensity observed for the STD effect was for methyl H4 bound to the sulfur atom was 100%. The relative STD effect of H5 methylene hydrogens had 98.2%.

3.3.2. Kinetic studies by NMR: determination of dissociation constant by STD

The determination of dissociation constant (K_D) was performed by the acquisition of STD experiments for each evaluated compound (**1a**,

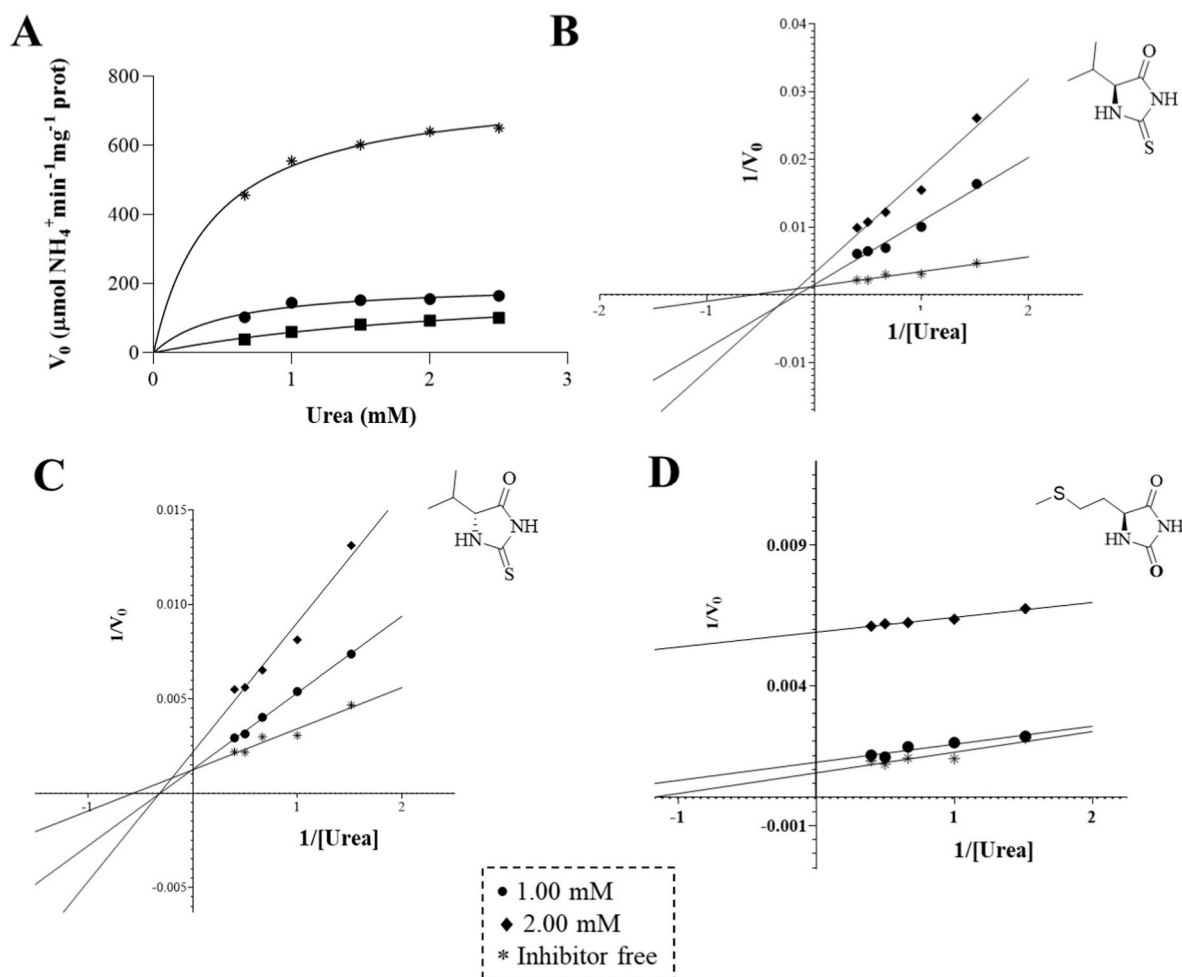


Fig. 2. (A) Exemplification of the Michaelis-Menten behavior of enzymatic catalysis of urease for **1b**. Urease inhibition mode from Lineweaver-Burk plots of the reciprocal of reaction rate vs. the reciprocal of the substrate (urea) in the absence (*) and in the presence of 2.00 mM (■) and 1.00 mM (●) of compounds **1b** (B), **1a** (C) and **2d** (D).

Table 4

Effect of thiohydantoin **1a**, **1b**, and **2d** on CEU kinetic parameters.

Amino acids	R ₂	R ₁		K _i (mM)	Alfa (α)	K _m (mM)	V _{max} (μmol/min ⁻¹)
D-val	(CH ₃) ₂ CH	H	1a	1.1 ± 0.3	2.7 ± 2	1.6 ± 0.3	788 ± 78
L-val	(CH ₃) ₂ CH	H	1b	0.4 ± 0.1	1.8 ± 1	1.6 ± 0.2	760 ± 49
L-met	CH ₃ S(CH ₂) ₂	H	2d	1.0 ± 0.2 [†]	–	0.6 ± 0.3	1076 ± 160

Values show the mean ± standard deviation of experiments performed in triplicate. Analysis of variance by the One-way ANOVA test found differences between all treatments with **p < 0.05 for **1a** and ****p < 0.0001 for **1b**, and **2d**. †AlphaK_i: Product between K_i and alpha value (also described as K_i[′]).

1b, and **2d**) at different concentrations, ranging from 0.20 to 2.00 mM (corresponding to 20 to 100-fold excess of ligand for each case) with fixed enzyme concentration (0.02 mM) (see more details on Supporting Information Figs. S20–21).

Thus, the titration based on the STD experiments provided the A_{STD} value corresponding to the protons that interacted effectively with the enzyme for each compound. The plots from Lineweaver-Burk graphics and correspondent linearization for methyl H1 and H2 from compounds **1a** and **1b**, and H4 from compound **2d** allowed us to estimate the K_D and αSTD (Fig. 6).

As can be observed in Table 5, compounds **2d** and **1b** presented the lowest K_D values of 1.26 and 1.79 mM, respectively, once again showing

to be the most active in the series of hydantoin and thiohydantoin evaluated. As expected, compound **1a** had the highest value of K_D = 3.00 mM (for colorimetric assay, K_i = 1.13 mM), also proving from this study that the S configuration of derivative **1b** is essential for interactions with CEU enzyme.

In order to observe quantitatively compared to results obtained from the colorimetric assays with the effects of the molecular interactions by STD, a Pearson Correlation Coefficient (r) analysis was performed on K_i and K_D data for the compounds **1a** and **1b**. The compound **2d** was not included in the analysis, since its constant is determined by the product between the K_i and the alpha parameter, thus the comparison with the K_D is not coherent.

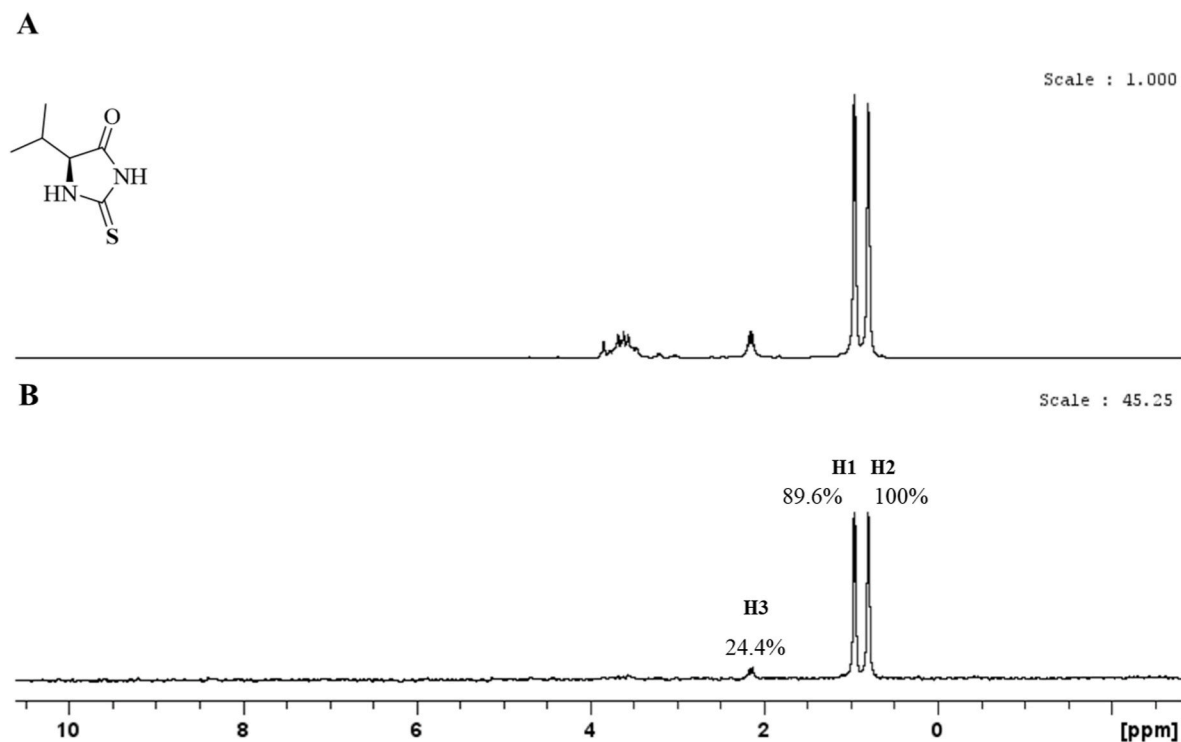


Fig. 3. NMR spectra of STD the experiment with assignment of ^1H signals from ligand **1b** with CEU. Reference spectrum (off-resonance) (**A**) and STD spectrum (**B**). Parameters: [CEU] = 0.02 mM; [**1b**] = 2.00 mM; phosphate buffer (in D_2O), pH 7.4; STD: Tsat = 1.5 s; Gauss1.1000 = 10 ms; Sync1.1000 = 2 ms; number of scans: 64.

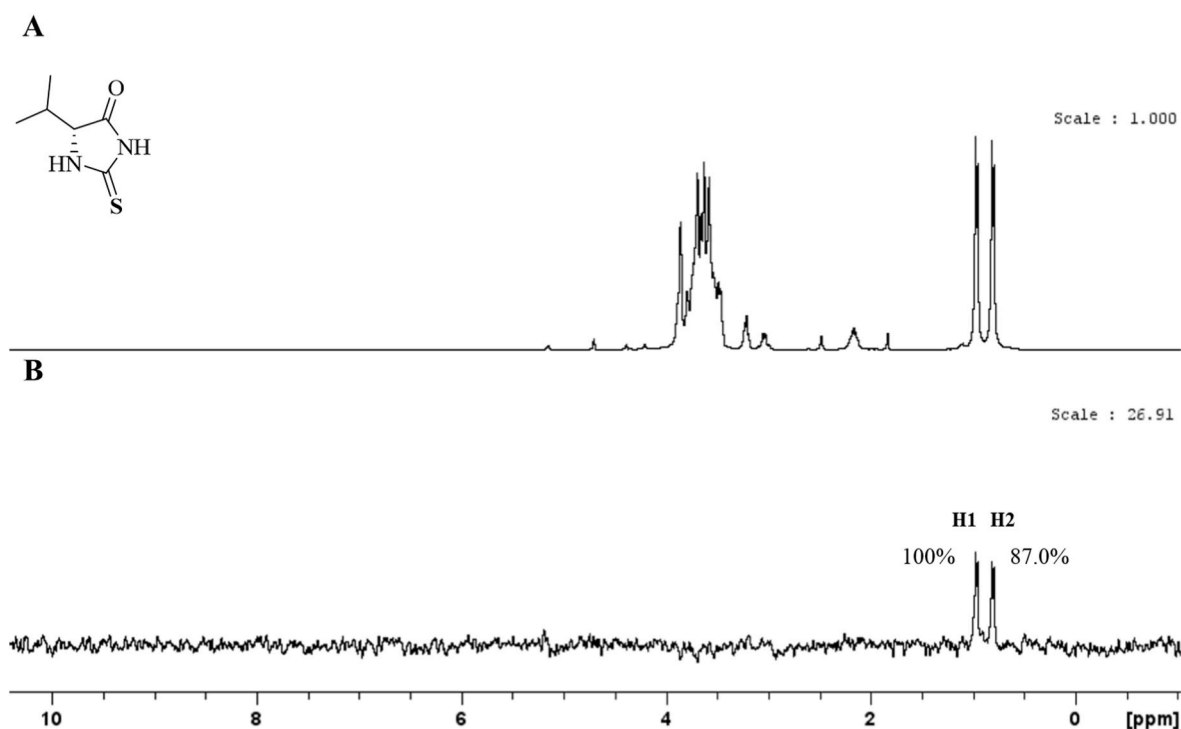


Fig. 4. NMR spectra of the STD experiment with assignment of the ^1H signals of ligand **1a** with CEU. Reference spectrum (off-resonance) (**A**) and STD spectrum (**B**). Parameters: [CEU] = 0.02 mM; [**1a**] = 2.00 mM; phosphate buffer (in D_2O), pH 7.4; STD: Tsat = 1.5 s; Gauss1.1000 = 10 ms; Sync1.1000 = 2 ms; number of scans: 64.

The coefficient r evaluates the linear correlation between two quantitative variables, being a dimensionless measure of covariance, with values of -1 to $+1$, where $r = 1$, indicates a perfect positive

correlation, $r = -1$ indicates a perfect negative correlation, and $r = 0$ indicates that there is no linear dependence on each other [36]. Noteworthy, the correlation analysis between the two variables of our

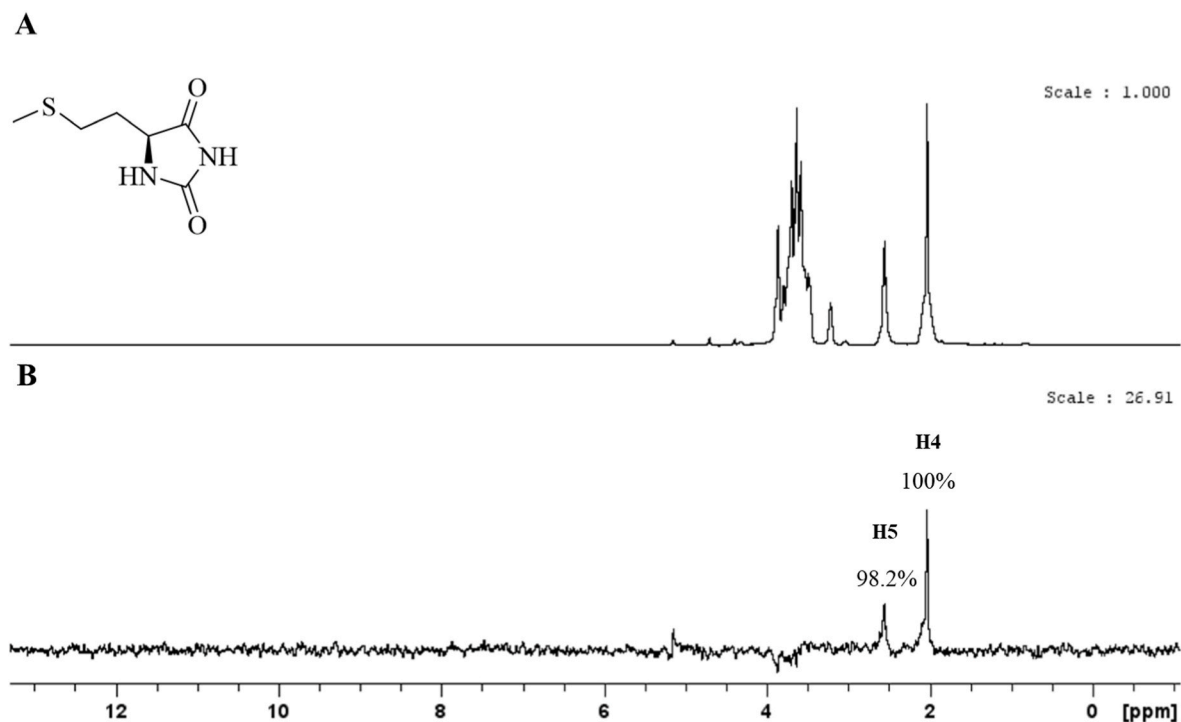


Fig. 5. NMR spectra from the STD experiment with assignment of the ^1H signals from the **2d** ligand with the CEU. Reference spectrum (off-resonance) (**A**) and STD spectrum (**B**). Parameters: [CEU] = 0.02 mM; [**2d**] = 2.00 mM; phosphate buffer (in D_2O), pH 7.4; STD: Tsat = 1.5 s; Gauss1.1000 = 10 ms; Sync1.1000 = 2 ms; number of scans: 64.

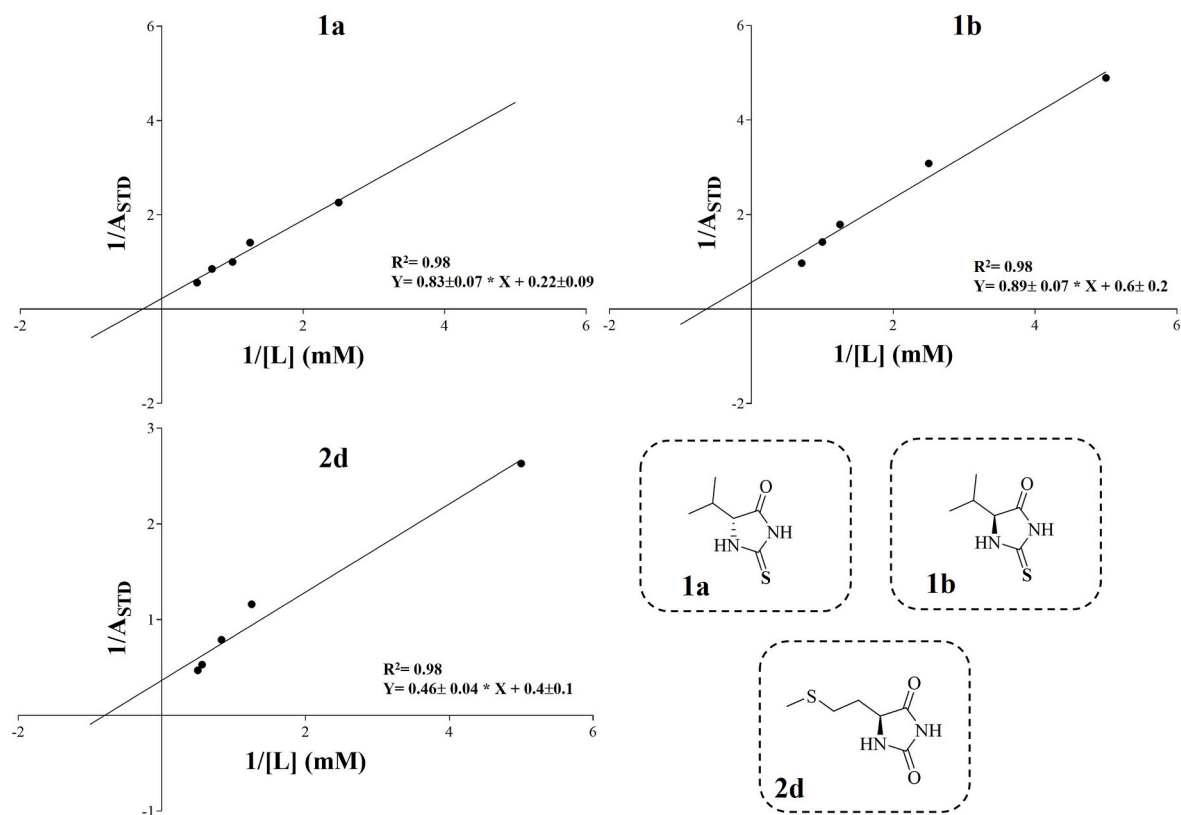


Fig. 6. Representative Lineweaver-Burk plots and their respective equations representing the slope and the ordinate at the origin with standard deviations of the lines for the methyl H1, H2, and H4, of compounds **1a**, **1b**, and **2d** respectively were used for the calculations of αSTD and K_D .

Table 5

Values of α_{STD} , K_D , and mean- K_D for all protons that showed STD effect of compounds **1a**, **1b**, and **2d** were evaluated.

Amino acids	Compound	H1		H2		H4 [†]		K_D^* (mM)
		α_{STD}	K_D (mM)	α_{STD}	K_D (mM)	α_{STD}	K_D (mM)	
D-val	1a	4.46	3.71	2.79	2.30	–	–	3.00
L-val	1b	1.90	2.02	1.77	1.57	–	–	1.79
L-met	2d	–	–	–	–	2.73	1.26	1.26

Data showed p -value < 0.005. [†]Methyl hydrogens bonded to the sulfur atom of hydantoin **2d**. • Mean- K_D , determined by the mean of all K_D values for the protons that showed the STD effect of each tested compound.

Table 6

Comparison between the constants K_i and K_D , by the Pearson correlation coefficient of compounds **1a** and **1b** evaluated.

Amino acids	R ₁	R ₂	Thiohydantoin	K_i mM (in vitro)	K_D mM (STD)	r
D-val	(CH ₃) ₂ CH	H	1a	1.13	3.00	1.00
L-val	(CH ₃) ₂ CH	H	1b	0.42	1.79	

studies (K_i and K_D) indicated an $r = 1.00$ (Table 6) (or 100%) which means a perfect positive correlation between these two variables for the investigated derivatives [37].

The calculated correlations suggest that the intermolecular ligand-to-enzyme contact pointed by the STD results is strictly related to the inhibitory activity measured for the analyzed derivatives.

3.4. Molecular docking studies

After *in vitro* evaluation by colorimetric assays and STD, molecular docking studies were carried out to obtain more information on the effects of thiohydantoin **1a**, **1b**, and hydantoin **2d** on the CEU (4H9M), evaluating their affinity for the active site of the enzyme and in an allosteric site.

The CEU monomer is subdivided into four domains, which resemble the shape of a hammer (Fig. 7): the N-terminal $\alpha\beta$ domain (1–134, in green) that connects to the β domain (286–401 and 702–761, in yellow) forming the “hammer handle” where this β domain is connected to two other $\alpha\beta$ domains, one of them the C-terminal domain (also called TIM-barrel domain) (402–701 and 762–840, in magenta) where is found the active site, and finally the $\alpha\beta$ domain (135–285, in red) forming the “hammerhead” (Fig. 7) [38]. The FTMap program mapped two possible interaction sites (see more details in the Supporting Information Section D), one being at the active site region (green sphere, Fig. 7), and the other at a site between the junction of the $\alpha\beta$ (1–134) and β (286–401, 702) domains –761) (red sphere, Fig. 7), in a deep cavity located in the

“hammer handle”.

The validation protocol chosen for the studies was redocking once several studies have shown it is usual to evaluate the accuracy of the docking procedure [39]. Therefore, we performed the redocking, and our protocol was validated with an RMSD value of 0.27 obtained by the ASP score function (Supporting Information, Fig. S22). In the first instance, we investigated the interaction of thiohydantoin **1a** and **1b** at the enzyme's active site since these compounds presented inhibitory profiles of the mixed type. Therefore, since hydantoin **2d** presented an uncompetitive inhibitory profile, it was not included in this molecular docking analysis. The mix type inhibition indicates that an inhibitor could interact in two steps: free enzyme (free-site) or enzyme-substrate complex when the inhibitor disturbs the substrate disconnection [40]. The co-crystallized acetohydroxamic acid (HAE) present at the active site of CEU (4H9M) is structurally similar to urea. In this way, we performed the docking simulations with the enzyme-inhibitor complex and without HAE (free-site) at the active site to check if the compounds could bind on the enzyme-substrate complex or free enzyme.

The molecular docking results at the free-site revealed that compounds **1a** and **1b** exhibited practically the same binding mode (Fig. 8E) and hydrophobic interactions with residues Arg439, Ala440, KCX490, Asp494, His519, His 545, Gly551, Gly550, His593, Asp633, Ala636, and Met637 (Fig. 8A and C). Furthermore, thiohydantoin **1b** presented a hydrogen bond between N1 of the thiohydantoin ring and His492, responsible for coordinating with Ni²⁺ and crucial for enzyme activity, which could explicate the high percentages of CEU inhibition by **1b** (90.5%) (Fig. 8A). For compound **1a** the hydrogen bond occurred also by the NH group, but the side chain extended spatially to the front (due to R-configuration) allowed interaction with Gly550 instead of His492, corroborating with the decrease of inhibition activity as observed on *in vitro* assays (27.8%) (Fig. 8C). Additionally, the sulfur atom coordinates with two Ni²⁺ ions at the free-site evaluated (Fig. 8A and C).

The number of interactions observed between the ligands and the free-site was much superior to the enzyme-HAE complex. Compounds **1a** and **1b** exhibited the same binding mode at the enzyme-inhibitor

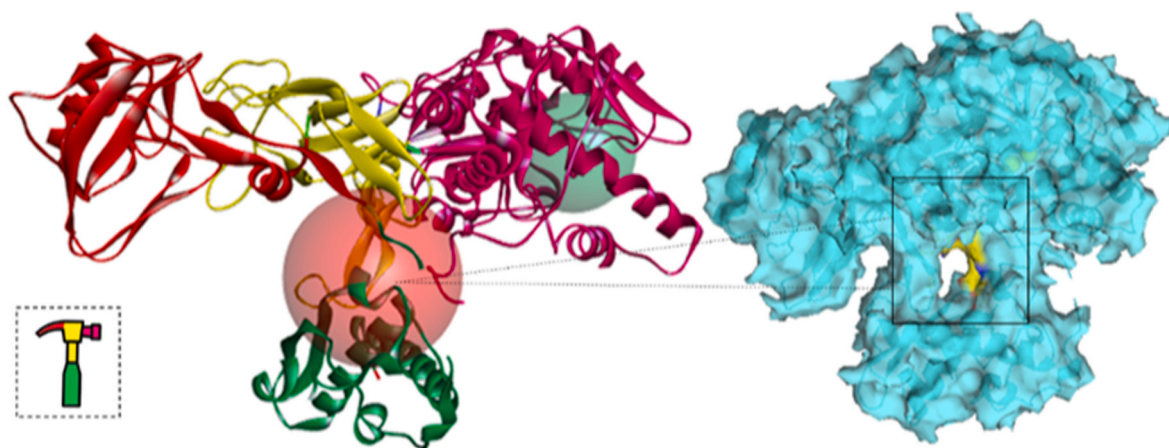


Fig. 7. Three-dimensional representation of the CEU monomer domains (PDB: 4H9M), and the possible interaction sites calculated by FTMap. The red sphere represents the allosteric site, and the green sphere the active site.

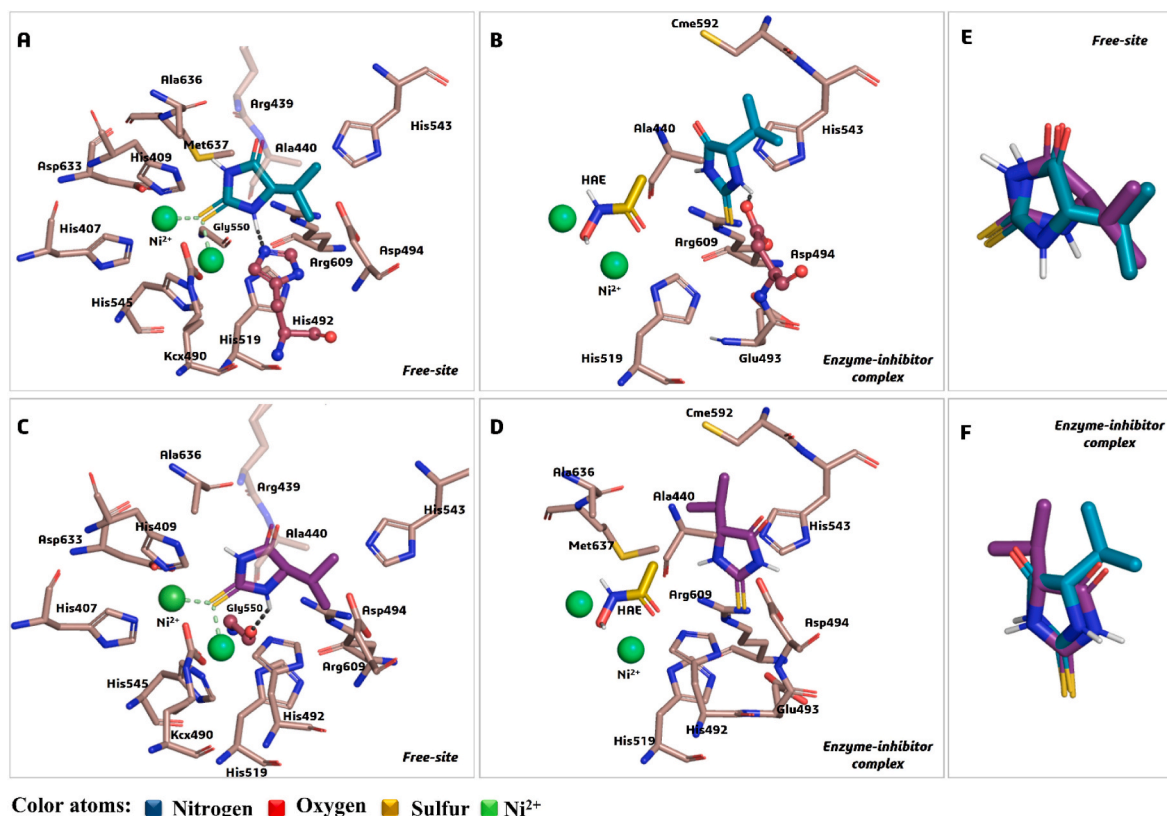


Fig. 8. Interaction diagrams of the best pose results of thiohydantoin at CEU free-site and enzyme-inhibitor complex (HAE, yellow). **1b** (blue): (A) and (B); **1a** (purple): (C) and (D). Overlap between ligands **1a** and **1b** at Free-site (E) and Enzyme-inhibitor-complex (F) are shown for best understanding. The dashed black lines represent the hydrogen-bonding interactions with amino acids (represented by spheres in burgundy color), and residues with hydrophobic interactions are represented by sticks in light burgundy color.

complex (Fig. 8F) and hydrophobic interactions with Ala440, His519, CME592, His593, Arg609, and Glu493. *R*-configuration of the thiohydantoin **1a** allowed interaction with Ala636. Additionally, they presented a hydrogen bond with Asp494 (Fig. 8B, D). Coordination with two Ni²⁺ was not observed since HAE occupied the space near the metal. These results agree with the experimental α values, which demonstrated that the thiohydantoin **1a** and **1b** have affinity by free enzyme,

since they presented $\alpha = 2.67$ and 1.83 , respectively.

The uncompetitive inhibitor **2d** can bind to allosteric sites; thus, other possible sites than the active one were mapped using the FTMap program (see more details in the Supporting Information Fig. S23).

The molecular docking results to **2d** are shown in Fig. 9, where we can observe the N1, N2 atoms, and oxygen from the thiohydantoin nucleus are involved in a hydrogen bond with Tyr32, Glu718, and Lys709,

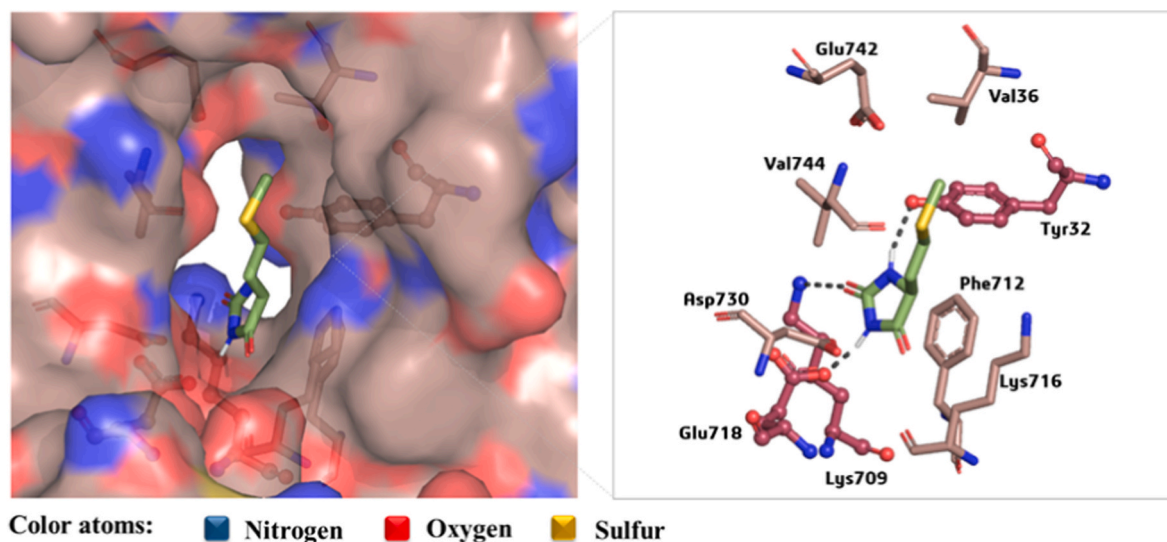


Fig. 9. Interaction diagrams of the best pose result of hydantoin **2d** (green) at CEU allosteric site. The dashed black lines represent the hydrogen-bonding interactions with amino acids (represented by spheres in burgundy color), and residues with hydrophobic interactions are represented by sticks in light burgundy color.

respectively. In addition, it was also possible to observe that the binding mode of this compound at the allosteric site of the enzyme allowed hydrophobic interactions with Val36, Phe712, Lys716, Asp730, Glu741, and Val744, since this compound has a more extensive aliphatic side chain, derived from methionine.

The binding mode of **2d** is in the middle of the *N*-terminal $\alpha\beta$ domain that connects to the β domain. This region is followed by the C-terminal ($\alpha\beta$) TIM barrel domain, which contains the active site, so the presence of an inhibitor in this local can compromise the enzymatic activity. Also was possible to note that the main interactions of **2d** were with Phe712, Lys709, Lys716, Glu718, Asp730, Glu741, and Val744, from the β domain which connects directly to the TIM barrel domain.

In general, the molecular docking results showed the crucial participation of the oxygen, sulfur, and N–H atoms of the thiohydantoin and hydantoin ring in the most critical binding interactions between the ligands and the target, indicating that this ring possibly acts as a pharmacophoric group in this series of compounds.

4. Conclusion

The study of CEU inhibition *in vitro* showed that the straightforward synthesized thiohydantoin have promising anti-ureolytic activities. The most active thiohydantoin **1b** and the hydantoin **2d** were identified as new hit inhibitors with, respectively, mixed, and uncompetitive inhibitory profiles.

Ligand-Enzyme interaction results demonstrated that saturated groups at the side chain of the amino acid residues of **1b** and **2d** have an important role in the binding to the macromolecular target. Besides, the absolute configuration of the antipodes **1a/1b** was crucial for the mode of binding with the enzyme. Finally, the findings suggest that oxygen, sulfur, and N–H participated in all hydrogen bond interactions with essential residues active or allosteric sites of the CEU enzyme, suggesting that the thiohydantoin and hydantoin rings can be considered pharmacophoric groups in these compounds.

Credit authorship contribution statement

- **Priscila Goes Camargo**: Conceptualization, methodology, formal analysis, investigation, writing.
- **Marciéli Fabris**: Methodology, formal analysis, investigation.
- **Matheus Yoshimitsu Tatsuta Nakamae**: Methodology, formal analysis, investigation.
- **Breno Germano de Freitas Oliveira**: Methodology, formal analysis, investigation.
- **Camilo Henrique da Silva Lima**: Supervision, software.
- **Ângelo de Fátima**: Supervision, resources, review and editing.
- **Marcelle de Lima Ferreira Bispo**: Review and editing, project administration, supervision.
- **Fernando Macedo**: Review and editing, project administration, supervision.

Funding

This work was made possible by the Network for the Development of Novel Urease Inhibitors (www.redniu.org) which is financially supported by the Brazilian agencies: Conselho Nacional de Desenvolvimento Científico e Tecnológico (CNPq), Coordenação de Aperfeiçoamento de Pessoal de Nível Superior (CAPES) and Fundação de Amparo à Pesquisa do Estado de Minas Gerais (FAPEMIG).

Declaration of competing interest

The authors declare that they have no known competing financial interests or personal relationships that could have appeared to influence the work reported in this paper.

Acknowledges

The authors gratefully acknowledge Dr. Mike P. Williamson (The University of Sheffield) for his helpful suggestion of the GEM-CRL approach. The authors would like to thank the Spectroscopy Laboratory (LABSPEC) NMR UEL/FINEP for the NMR experiments.

Appendix A. Supplementary data

Supplementary data to this article can be found online at <https://doi.org/10.1016/j.cbi.2022.110045>.

References

- [1] B. Krajewska, Ureases I. Functional, catalytic and kinetic properties: a review, *J. Mol. Catal. B Enzym.* 59 (2009) 9–21, <https://doi.org/10.1016/j.molcatb.2009.01.003>.
- [2] S.J. Lippard, *At Last-The Crystal Structure of*, 1995, p. 268.
- [3] J.C. Polacco, M.A. Holland, Roles of urease in plant cells, *Int. Rev. Cytol.* 145 (1993) 65–103, [https://doi.org/10.1016/S0074-7696\(08\)60425-8](https://doi.org/10.1016/S0074-7696(08)60425-8).
- [4] W.A.R.L. Cabezas, G.H. Korndorfer, S.A. Motta, Volatilização de N-NH₃ na cultura de milho: II. avaliação de fontes sólidas e fluidas em sistema de plantio direto e convencional, *Rev. Bras. Ciência do Solo* 21 (1997) 489–496, <https://doi.org/10.1590/s0100-06831997000300019>.
- [5] B. Beig, M.B.K. Niazi, Z. Jahan, A. Hussain, M.H. Zia, M.T. Mehran, Coating materials for slow release of nitrogen from urea fertilizer: a review, *J. Plant Nutr.* 43 (2020) 1510–1533, <https://doi.org/10.1080/01904167.2020.1744647>.
- [6] H. Cantarella, P.C.O. Trivelin, T.L.M. Contín, F.L.F. Dias, R. Rossetto, R. Marcelino, R.B. Coimbra, J.A. Quaggio, Ammonia volatilisation from urease inhibitor-treated urea applied to sugarcane trash blankets, *Sci. Agric.* 65 (2008) 397–401, <https://doi.org/10.1590/S0103-90162008000400011>.
- [7] M.J. Maroney, S. Ciurli, Nonredox nickel enzymes, *Chem. Rev.* 114 (2014) 4206–4228, <https://doi.org/10.1021/cr4004488>.
- [8] Y.F. Rego, M.P. Queiroz, T.O. Brito, P.G. Carvalho, V.T. de Queiroz, Â. de Fátima, F. Macedo, A review on the development of urease inhibitors as antimicrobial agents against pathogenic bacteria, *J. Adv. Res.* 13 (2018) 69–100, <https://doi.org/10.1016/j.jare.2018.05.003>.
- [9] A. Pilotto, M. Franceschi, *Helicobacter pylori* helicobacter pylori infection in older people, *World J. Gastroenterol.* 20 (2014) 6364–6373, <https://doi.org/10.3748/wjg.v20.i21.6364>.
- [10] T.O. Brito, A.X. Souza, Y.C.C. Mota, V.S.S. Moraes, L.T. De Souza, Â. De Fátima, F. Macedo, L.V. Modolo, Design, syntheses and evaluation of benzoylthioureas as urease inhibitors of agricultural interest, *RSC Adv.* 5 (2015) 44507–44515, <https://doi.org/10.1039/c5ra07886e>.
- [11] Z.D. Wang, S.O. Sheikh, Y. Zhang, A simple synthesis of 2-thiohydantoin, *Molecules* 11 (2006) 739–750, <https://doi.org/10.3390/11100739>.
- [12] T.R. Fagundes, B. Bortoleti, P. Camargo, V. Concato, F. Tomiotto-Pellissier, A. Carlotto, C. Panis, M. Bispo, F.M. Junior, I. Conchon-Costa, W. Pavanelli, Patterns of cell death induced by thiohydantoin in human MCF-7 breast cancer cells, *Anti Cancer Agents Med. Chem.* (2021), <https://doi.org/10.2174/1871520621666210811102441>.
- [13] J. Marton, J. Enisz, S. Hosztafi, T. Tímár, Preparation and fungicidal activity of 5-substituted hydantoin and their 2-thio analogs, *J. Agric. Food Chem.* 41 (1993) 148–152, <https://doi.org/10.1021/jf00025a031>.
- [14] P.G. Camargo, M. Fabris, T.U. Silva, C.H. Silva Lima, S. Paula Machado, L.T. D. Tonin, M. Lima Ferreira Bispo, F. Macedo, Thiohydantoin as potential antioxidant agents: in vitro and in silico evaluation, *ChemistrySelect* 6 (2021) 10429–10435, <https://doi.org/10.1002/slct.202102840>.
- [15] P.G. Camargo, B.T. da S. Bortoleti, M. Fabris, M.D. Gonçalves, F. Tomiotto-Pellissier, I.N. Costa, I. Conchon-Costa, C.H. da S. Lima, W.R. Pavanelli, M. de L. F. Bispo, F. Macedo, Thiohydantoin as anti-leishmanial agents: n vitro biological evaluation and multi-target investigation by molecular docking studies, *J. Biomol. Struct. Dyn.* (2020) 1–10, <https://doi.org/10.1080/07391102.2020.1845979>, 0.
- [16] B. Taciane da Silva Bortoleti, M.D. Gonçalves, F. Tomiotto-Pellissier, P.G. Camargo, J.P. Assolini, V.M. Concato, M.B. Detoni, D.L. Bidóia, M. de Lima Ferreira Bispo, C. Henrique da Silva Lima, F. Cesar de Macedo, I. Conchon-Costa, M.M. Miranda-Sapla, P.F. Wowk, W.R. Pavanelli, Investigation of the antileishmanial activity and mechanisms of action of acetyl-thiohydantoin, *Chem. Biol. Interact.* 351 (2021), 109690, <https://doi.org/10.1016/j.cbi.2021.109690>.
- [17] P.G.C. de Carvalho, J.M. Ribeiro, G. Nakazato, R.P.B. Garbin, S.F.Y. Ogatta, Â. de Fátima, M.L.F. Bispo, F. Macedo Jr., Synthesis and antimicrobial activity of thiohydantoin derived from L-amino acids, *Lett. Drug Des. Discov.* 16 (2018), <https://doi.org/10.2174/1570180816666181212153011>.
- [18] J. Schörhuber, T. Sára, M. Bisaccia, W. Schmid, R. Konrat, R.J. Lichtenegger, Novel approaches in selective tryptophan isotope labeling by using *Escherichia coli* overexpression media, *Chembiochem* 16 (2015) 746–751, <https://doi.org/10.1002/cbic.201402677>.
- [19] S. Reyes, K. Burgess, On formation of thiohydantoin from amino acids under acylation conditions, *J. Org. Chem.* 71 (2006) 2507–2509, <https://doi.org/10.1021/jo052576i>.
- [20] J.A. Khan, A. tul Wahab, S. Javaid, M. Al-Ghamdi, E. Huwait, M. Shaikh, A. Shafqat, M.I. Choudhary, Studies on new urease inhibitors by using biochemical,

- STD-NMR spectroscopy, and molecular docking methods, *Med. Chem. Res.* 26 (2017) 2452–2467, <https://doi.org/10.1007/s00044-017-1945-3>.
- [21] T. Parella, Pulse program catalogue : experiments, *Pulse Progr. Cat* (2006) 1–249.
- [22] Atta-ur Rahman, M.I. Choudhary, Atia-tul-Wahab, Solving Problems with NMR Spectroscopy, Elsevier, 2016, <https://doi.org/10.1016/C2012-0-06253-9>.
- [23] T.D.W. Claridge, High-Resolution NMR Techniques in Organic Chemistry, Elsevier, 2016, <https://doi.org/10.1016/C2015-0-04654-8>.
- [24] D. Systèmes, Biovia Discovery Studio ® 2016 Comprehensive Modeling and Simulations, 2016.
- [25] W.L. DeLano, Pymol: an open-source molecular graphics tool, *CCP4 Newsl. Protein Crystallogr.* 40 (2002) 82–92.
- [26] O. Korb, T. Stützel, T.E. Exner, An ant colony optimization approach to flexible protein–ligand docking, *Swarm Intell* 1 (2007) 115–134, <https://doi.org/10.1007/s11721-007-0006-9>.
- [27] Z. Huang, C.S. Ough, Determination of amino acid hydantoins by HPLC with diode array detection, *J. Agric. Food Chem.* 39 (1991) 2206–2213, <https://doi.org/10.1021/jf00012a023>.
- [28] R.A. Copeland, Evaluation of enzyme inhibitors in drug discovery. A guide for medicinal chemists and pharmacologists, *Methods Biochem. Anal.* 46 (2005) 1–265.
- [29] A. Viegas, J. Manso, F.L. Nobrega, E.J. Cabrita, Saturation-transfer difference (STD) NMR: a simple and fast method for ligand screening and characterization of protein binding, *J. Chem. Educ.* 88 (2011) 990–994, <https://doi.org/10.1021/ed101169t>.
- [30] S. Kemper, M.K. Patel, J.C. Errey, B.G. Davis, J.A. Jones, T.D.W. Claridge, Group epitope mapping considering relaxation of the ligand (GEM-CRL): including longitudinal relaxation rates in the analysis of saturation transfer difference (STD) experiments, *J. Magn. Reson.* 203 (2010) 1–10, <https://doi.org/10.1016/j.jmr.2009.11.015>.
- [31] A. Wahab, A. Khan, B.P. Marasini, M.A. Lodhi, A. Rahman, M.I. Choudhary, Discovery and study of the binding epitopes of Novel urease inhibitors by STD-NMR spectroscopy and biochemical analyses, *Lett. Drug Des. Discov.* 10 (2013) 515–521, <https://doi.org/10.2174/1570180811310060007>.
- [32] J.A.J. Awllia, A. Sara, A. Wahab, M. AL-Ghamdi, S. Rasheed, E. Huwait, M. Iqbal Choudhary, Discovery of new inhibitors of urease enzyme: a study using STD-NMR spectroscopy, *Lett. Drug Des. Discov.* 12 (2015) 819–827, <https://doi.org/10.2174/1570180812666150520001629>.
- [33] M.P. Williamson, Chapter 3 Applications of the NOE in Molecular Biology, first ed., Elsevier Ltd, 2009 [https://doi.org/10.1016/S0066-4103\(08\)00203-2](https://doi.org/10.1016/S0066-4103(08)00203-2).
- [34] J.L. Sorge, J.L. Wagstaff, M.L. Rowe, R.A. Williamson, M.J. Howard, Q2DSTD NMR deciphers epitope-mapping variability for peptide recognition of integrin $\alpha v \beta 6$, *Org. Biomol. Chem.* 13 (2015) 8001–8007, <https://doi.org/10.1039/C5OB01237F>.
- [35] S. Chu, G. Zhou, M. Gochin, Evaluation of ligand-based NMR screening methods to characterize small molecule binding to HIV-1 glycoprotein-41, *Org. Biomol. Chem.* 15 (2017) 5210–5219, <https://doi.org/10.1039/C7OB00954B>.
- [36] H.A. Miot, Correlation analysis in clinical and experimental studies, *J. Vasc. Bras.* 17 (2018) 275–279, <https://doi.org/10.1590/1677-5449.174118>.
- [37] P. Schober, L.A. Schwarte, Correlation coefficients: appropriate use and interpretation, *Anesth. Analg.* 126 (2018) 1763–1768, <https://doi.org/10.1213/ANE.0000000000002864>.
- [38] A. Balasubramanian, K. Ponnuraj, Crystal structure of the first plant urease from Jack bean: 83 Years of journey from its first crystal to molecular structure, *J. Mol. Biol.* 400 (2010) 274–283, <https://doi.org/10.1016/j.jmb.2010.05.009>.
- [39] R.E.L. Kirk, E. Hevener, Wei Zhao, David M. Ball, Kerim Babaoğlu, Jianjun Qi, Stephen W. White, Validation of molecular docking programs for virtual screening against dihydropteroate synthase, *J. Chem. Inf. Model.* 49 (2) (2009) 1–7.
- [40] M.O. Sousa, T.L.S. Miranda, E.B. Costa, E.R. Bittar, M.M. Santoro, A.F. S. Figueiredo, Linear competitive inhibition of human tissue kallikrein by 4-aminobenzamidine and benzamidine and linear mixed inhibition by 4-nitroaniline and aniline, *Braz. J. Med. Biol. Res.* 34 (2001) 35–44, <https://doi.org/10.1590/S0100-879X2001000100004>.